Proceedings of TMCE 2014, May 19-23, 2014, Budapest, Hungary, Edited by I. Horváth, Z. Rusák
© Organizing Committee of TMCE 2014, ISBN 978-94-6186-177-1

RECOGNITION OF THIN FEATURES USING HEAT DIFFUSION

Ramy Harik
Department of Industrial and Mechanical Engineering
Lebanese American University
Lebanon
ramy.harik@gmail.com

Alexandre Durupt
Department of Mechanical Systems Engineering,
Université de Technologie de Compiègne,
Compiègne, 60203, France
alexandre.durupt@utc.fr

Joe Khalifeh
Department of Electrical and Computer Engineering
Lebanese American University
Lebanon
joe.khalifeh@lau.edu

Benoit Eynard
Department of Mechanical Systems Engineering,
Université de Technologie de Compiègne,
Compiègne, 60203, France
benoit.eynard@utc.fr

ABSTRACT

This paper investigates a novel approach to recognize thin features. The latter are primary for planning the manufacturing setup in aircraft industries. Traditional techniques survey geometrical variations to detect their presence. Through this article, we will present a new detection technique using a combination between heat diffusion and persistence homology. This will serve to recognize typical heat diffusion protrusions and to classify them accordingly.

KEYWORDS

Thin Features, Shape matching, persistence, heat kernel, feature recognition

1. INTRODUCTION

Mechanical parts, in aircraft industries, join the most contradicting design requirements: high strength and low weight. This generates the abundant presence of a particular mechanical feature: Thin Features. In the following introduction, we first present thin features, then, we detail the upcoming sections in this article.

1.1. Thin Features

Thin features refer to traditional protrusion and pocket features with a particular attribute: thickness to height ratio is relatively low forcing a particular manufacturing setup.

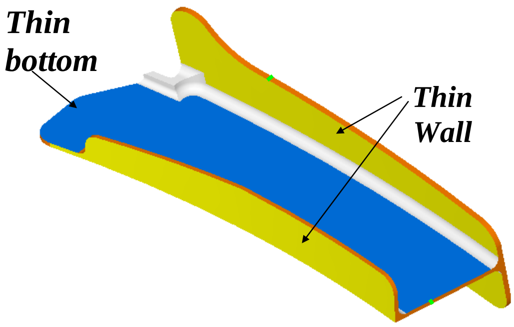

Figure 1. Thin Features

Figure 1 presents a typical aircraft part, used in [1]. Thin features can be classified into two distinct types: Thin walls and Thin Bottoms. The manufacturing fixtures, refer to Figure 2, heavily influence the typology of a feature. As this article does not handle the automated selection of a manufacturing fixture, we attempt to classify thin features at large. The importance of properly identifying which sub feature type finds its roots in setting up an appropriate manufacturing program. Thin walls are manufacturing through the alternation of the manufacturing side along the same direction as shown in Figure 3. Thin bottoms might require strengthening the base to avoid deflection.

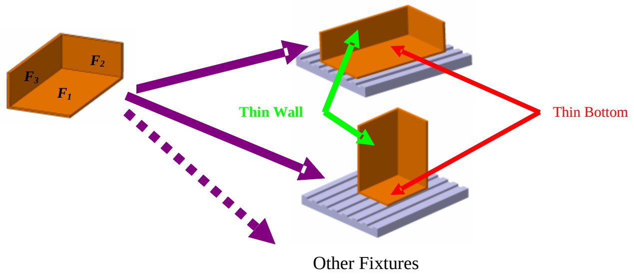

Figure 2. Fixtures and their effect on the sub type

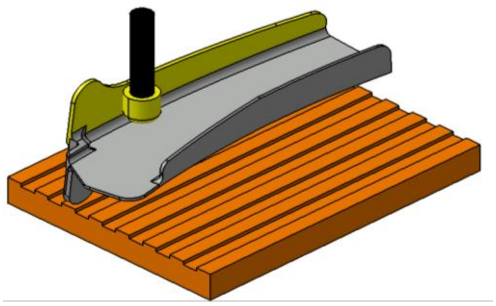

Figure 3. Peculiar manufacturing of a thin feature

1.2. Structure

The following sections of the article will first introduce a state of the art. The latter is split into two components: one relevant to traditional works investigating the identification of thin features, the second related to the more recent techniques using persistence homology and heat diffusion. Then, section three, presents a previous methodology, relying on geometrical computations, used to identify thin features. Section four presents the novel technique reaping the benefits of persistence homology and feature identification. The article ends up with a conclusion and perspective for future works.

2. STATE OF THE ART

Related works deal with setting up proper milling conditions of thin walls. Typically, they investigate stability analysis during the milling process by the cutting forces using FEM (Finite Element Model) method for machining simulation.

As an example, [2] propose a methodology to determine the stability or the instability of thin walls during manufacturing. The approach covers all stages of the thin wall milling and is based on the cutting forces analysis. More recently, [3] present a mathematical model of FEM for corners milling detection of thin walled cavities on aeronautical components. [4] propose an overview of a FEM method based milling process plan verification model and associated tools. Their method allows a machining simulation for analysing part errors, induced during milling of thin-walled components.

The industrial challenge is to reduce both cost and manufacturing time. For this, we consider that the thin wall detection should be identified at the design stage rather than the process planning one.

2.1. Thin wall manufacturing and identification

A large overview of related works based on thin wall detection at the design stage is proposed below.

For the aeronautic context, the project HITHRU III [5] deals with process planner assistance. The problem of thin wall detection is highlighted but the CIMSKILL software does not to detect it.

The project MADEsmart [6] is dedicated to the multidisciplinary optimization and integration of manufacturing constraints in design stage for spare aeronautic parts. Three main technologies to improve the design of aircraft parts are used : (1) the multi agent system to coordinate the resources between teams of development; (2) MDO (Multidisciplinary design optimization) to solve design problems incorporating a number of disciplines; (3) the LCS (Lexical Conceptual Structure) in order to introduce a semantically representation of constraints in design stage. The manufacturability analysis is as well ensured by CIMSKILL. The latter includes a database of standards on milling aluminum and titanium parts. A database of 5-axis milling features and a library of cutting tools had been added. This system is able to detect 80% of features of the parts but does not detect complex or specific features, such as thin walls.

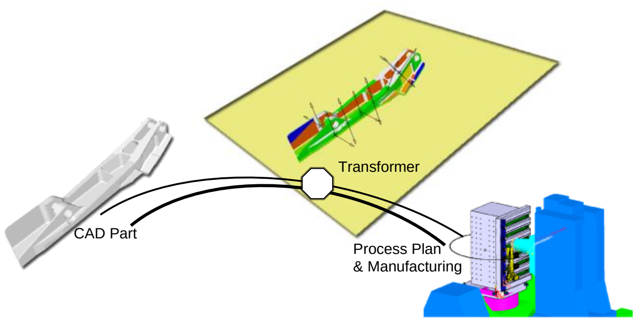

Figure 4. USIQUICK by [7]

The French National Project USIQUICK [7], which ended in 2006, had to provide a software for manufacturing parts in the aeronautical domain. The creating of automatic process plan, selection of the cutting tools, optimization of the fixtures as well as the automatic tool path generation with documentation are functionalities of USIQUICK. The input of the system is a CAD part and the outputs are support functions and documentation for the process planner. The system is split in three main modules such as the “Transformation”, the “Preparation” and “Generation”. The “Transformation” is used to adapt the geometry of the CAD model for the preparation model. The “Preparation” is used to obtain a Macro process consisted of fixtures and tools. The “Generation” calculates the tool paths and provides a milling simulation. The CNC G-code is next generated with documentation on milling strategies. The manufacturing analysis is mainly ensured by the “transformation” module. The thin wall detection is one of the functionalities suggested by the system.

For other domains, Zhao [8], in their work on manufacturing analysis of sheet metal and injecting parts, relate the problem of thin wall detection. The authors specify that such peculiar features do not exist in typical databases.

[9] developed an approach to evaluate the manufacturing analysis of foundry parts in order to ensure the parts are compatible with a manufacturing process. Their work propose an algorithm based on three concepts : (1) the orientation of parts and tools ; (2) the determination of edges, thin wall, ribs ; (3) the addition of chamfers, filets, circular edges, and draft surfaces to adapt the part with a manufacturing process. The evaluation is made by features' extraction such as plan surfaces and concave areas. Thus, their work allows detecting simple thin wall on prismatic parts milled in 3-axis machine.

To summarize, scientific literature contains several works associated with thin wall detections in CAD/CAPP/CAM systems, where the activity of process planer is often situated between CAD and CAM environments. This activity demands complex brainstorming. The time needed to establish a correct process plan range between 5 to 20 days for complex parts. Since aeronautical industries do not mass produce, we assume that the brainstorming time has to be reduced. The thin wall detection will allow reducing the process planning time.

2.2. Persistence heat signature

Shape recognition performed through heat is achieved by solving the heat equation over the geometry. [10] shows that the solution of the heat equation called the heat kernel is related to the eigenvalues and eigenfunctions of the Laplacian. The use of the Laplace operator along with the heat kernel is used to discover geometrical information about the manifolds. The link between the analysis of the geometry and the geometry itself is the eigenvalues of the Laplace operator. [11] develops an algorithm that approximates the Laplace operator on a meshed surface with point-wise convergence. The algorithm was empirically proved to exhibit convergence and outperforms other methods in accuracy and robustness with respect to noise data. [12] shows that the synergy between HKS and persistent homology leads to an efficient pose-oblivious matching algorithm that can be used for all models, whether partial, incomplete, or complete. The matching of partial and incomplete models cannot rely on global features. However any matching relying on only local features becomes susceptible to noise caused by small perturbations. Using small time scales to match local features increases the local variation in the HKS function values making it more sensitive to noise. To overcome this problem, persistent homology was introduced. Candidates for feature points are considered to be the maxima of the HKS which persist beyond a given threshold. Instead of detecting the persistence of all critical values, the implemented algorithm eliminates maxima that are not persistent. Experimental results show that this method is effective in shape matching. The heat kernel may be used to perform other geometrical applications other than shape recognition. One of these applications is 3D mesh segmentation. [13] states that isometrically-variant segmentation of the surface, sensitivity to topological perturbations of the surface, sensitivity to numerical noise and inconsistency with human understanding of segmentation are problems that a segmentation approach confronts. A novel approach is introduced dealing with perceptually consistent mesh segmentation (PCMS) by exploring heat kernel featured space to which the geometric features of mesh are mapped. PCMS provides a solution for the problems of segmentation. Shape signature is a concise representation of the shape that captures some of its essence. It could be used in various applications such as 3D shape similarity.

Since many shapes manifest rich variability, shape retrieval is often required to be invariant to different classes of transformations and shape variations such as scale variance, orientations, missing data, and appearance in different formats and representations [14].

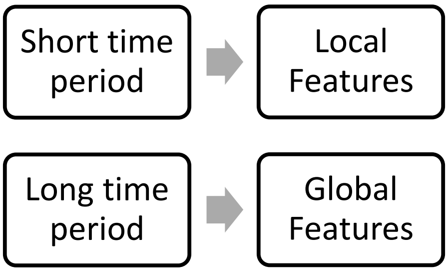

Figure 5. HKS and feature recognition

The Heat Kernel Signature is a widely used signature. The use of HKS at different time values allows the description of features at multiple scales. The synergy between HKS and persistent homology leads to an efficient pose-oblivious matching algorithm that can be used for all models, whether partial, incomplete, or complete.

3. USIQUICK'S METHODOLOGY FOR THIN WALL DETECTION

This section shows the USIQUICK method based on feature extraction from a CAD model. To start, we explain the process plan rules modeling, next the algorithms and detections results.

3.1. Modeling of process planner rules to analyze thin walls

In the aeronautical domain, the process planner defines the main fixture plan of the part. Then, he measures the length from some preselected points on a presumed thin wall. Next, the height h and thickness ε_R are measured. The assumed wall is considered a Thin Wall if at least one measure point respects the following condition.

$$\frac{h}{\varepsilon_R} < \lambda \quad (1)$$

The ratio λ depends of the material but for this paper, λ is considered between 5 and 8. This framework comes from the expertise of aeronautical process planners.

3.2. Usiquick's algorithm

The suggested algorithm below is to detect the CAD faces of a thin wall. The process is mainly based on the comparison between real thicknesses of the model and the thickness calculated from the expert rule (1).

A face of the model is considered as well as neighbouring surfaces. Only faces milled according to flank or end modes with adjacent thin faces will be eligible. Thus, eligibility is based on two main steps: (1) the study of surfaces with thin boundary edges; (2) the study of the thickness.

The eligibility surfaces are often semi-opened containing several open edges.

From the analysis of some aeronautical parts, it appears that the surfaces where the sum of lengths of opened edges lgO is over 75% perimeter P are analyzed:

$$\lg O \geq 0.75 \times P \, (2)$$

Rule (2) allows to eliminate fillets of the part and the flank surfaces of the thin wall and to detect the thin top of the walls.

Following, we determine the thickness of the wall. For this, we consider that the geometrical shape is called "thick" when its length is more than its width. The easier criterion is to compare the length with the width. However, with complex surfaces, this criterion is not measurable (see Figure 6).

Figure 6. Assimilation of complex surfaces to rectangular ones

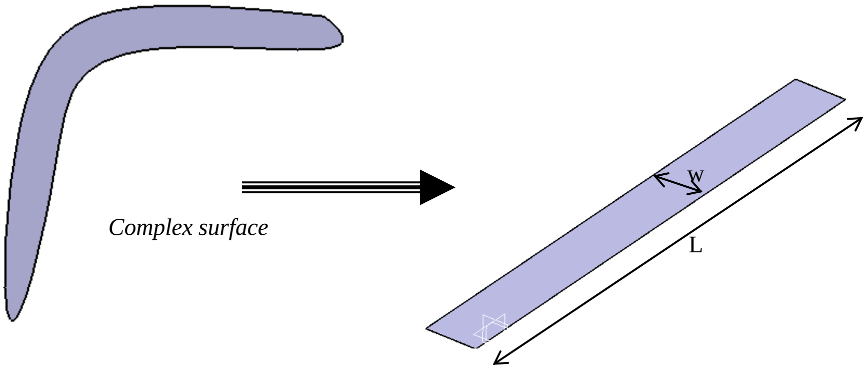

To overcome this issue, we assimilated complex surfaces and made it possible to estimate the ratio between the length (L) and Width (w) according to the surfaces (S) and the perimeter (P).

$$P = 2(L+w) \Rightarrow \frac{P^2}{4} = w^2 + 2Lw + w^2 \quad (3)$$

$$\frac{P^2}{4} = L^2 + 2Ll \quad (4)$$

$$\frac{P^2}{4S} = \frac{L^2 + 2Lw}{S} = \frac{L^2}{Lw} + \frac{2Lw}{Lw} = \frac{L}{w} + 2 \quad (5)$$

$$\frac{L}{w} = \frac{P^2}{4S} - 2 \quad (6)$$

This ratio (6) allows characterizing the thickness of a surface. A high value confirms that a surface is not a square shape.

Following several computation, we were able to deduct the below condition (7) to consider a feature as a thin feature.

$$\begin{cases} \text{If : } P_s < P_{sav} \quad \text{then : } \dfrac{L}{w} \geq 5 \\ \qquad\qquad \textit{and} \qquad\qquad\qquad (7) \\ \text{If : } P_s \geq P_{sav} \quad \text{then : } \dfrac{L}{w} \geq 5 \times e^{(100 \times (P_s - P_{sav}))} \end{cases}$$

The limit and condition expressed above are deducted from a test led on 8 aeronautical parts.

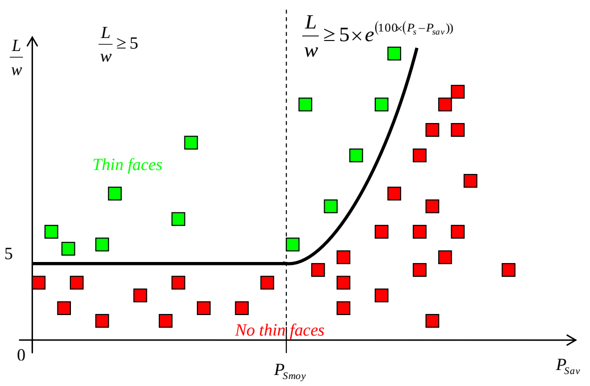

Figure 7. Equation deduction following manual classification of thin features.

4. PERSISTENT HEAT SIGNATURE

This section presents the adopted methodology to recognize thin features. The proposed solution joins two algorithms that are briefly prescribed below:

- Algorithm 1: Using persistence homology to recognize potential protrusion features. This work is shallowly detailed in this publication.
- Algorithm 2: Generating a thinness probability to identify most probable thin features. This builds on the previous results in algorithm 1.

Following the presentation of both algorithms, we forward a section showing current results.

4.1. Recognition of protrusions

The following paragraph describes the approach adopted to recognize protrusions and pocketed features. It follows the digital detection logic of RIMA (RecognItion and feature MAtching). RIMA is an application developed in Matlab ®.

Input can be an '.off' file or a CATIA ® mesh resulting '.dat' file. Ideally, the software can be connected to other attempts at treating cloud of points obtained from a 3D scanning device and have its noise filtered and triangulation performed. **Error! Reference source not found.** shows the two traditional input methods leading to delivering a triangulated mesh. The latter is the input of RIMA. Different mesh sizes were tried (10mm, 5mm, 1mm…) as well as non uniform and uniform meshing. Refining our mesh would certainly lead to more accurate results however in the expense of computation time. 2mm uniform mesh gave good results while being not expensive.

Stage 1: Heat Kernel Signature

Throughout this stage, we attempt to estimate the heat losses a source endures through time. The rate, at which a source diffuses heat, is deemed an indicator on the localization of a point with respect to its surroundings. In order to do so, we attempt to solve the partial differential diffusion equation used on a compact Riemannian manifold. Figure 8 shows heat diffusion on a part after application of a unit heat at the tip of the sphere applied within RIMA at different time intervals.

$$\frac{\delta U}{\delta t} - \kappa \nabla^2 U = 0$$

Equation 1. Partial differential diffusion equation

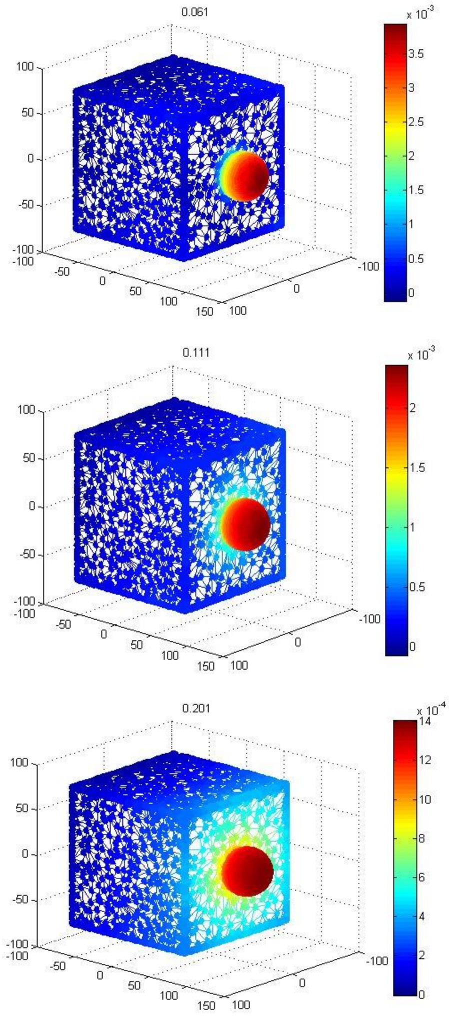

Figure 8. Heat diffusion when a source heat is applied at t=0.061, t=0.111, t=0.201

A known solution for Equation 1 is the heat kernel. The heat kernel represents the quantity of heat received by a point after a unit of heat is applied at a certain reference point at time t=0. The amount of heat is computed for discrete cases using Equation 2. Parameters λ and φ are the eigenvalues and eigenvectors solution to the Laplacian Matrix. The first 300 values are considered.

$$H_t(x, y) = \sum_{i=1}^{300} e^{-\lambda_i t} \phi_i(x)\phi_i(y)$$

Equation 2. Heat Kernel

We use a modified Laplacian in the application of the heat kernel. While regularly matrices tend to include an indicator to the manifold curvature – the cotangent –, we add a mesh uniformity factor to overcome mesh proportionality and skewness. This weight applied to the traditional cotangent value is exhibited by the Voronoi area. Equation 3 presents our modification of the Laplacian. Figure 9 presents the geometric elements needed for the equation.

$$L_{ij} = \frac{1}{S_i}\left(\frac{\cot \alpha_{ij} + \cot \beta_{ij}}{2}\right)$$

Equation 3. Normalized cotangent

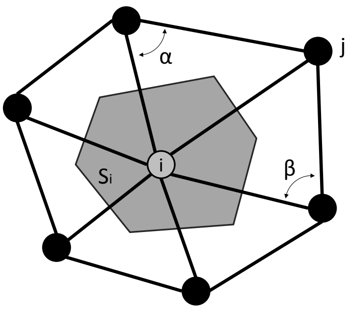

Figure 9. Geometric elements to compute the modified normalized Laplacian

RIMA gives the ability to specify the time frame and the desired computation steps. Standard values are from t=0.001 to t=1, using a 0.001 step (τ). At each instance t, heat retained at the source H is computed and saved in a HKS record matrix. Each point of the starting block is treated separately and used to complete the HKS record. This step is the most expensive computationally. The computation time can be further refined through usage of model reduction techniques.

At the end of this stage we would have for each point the amount of heat retained as time elapses.

Stage 2: Computing the local heat persistence level and value

This second stage will measure the persistence P of a point to retain heat and to resistant losing its heat. Heat persistence is defined an interval where the heat value on a node persists above a minimum threshold. Persistence could be calculated by level or by value. We will thus apply persistence homology to extract significant subsets of the global mesh at different time intervals.

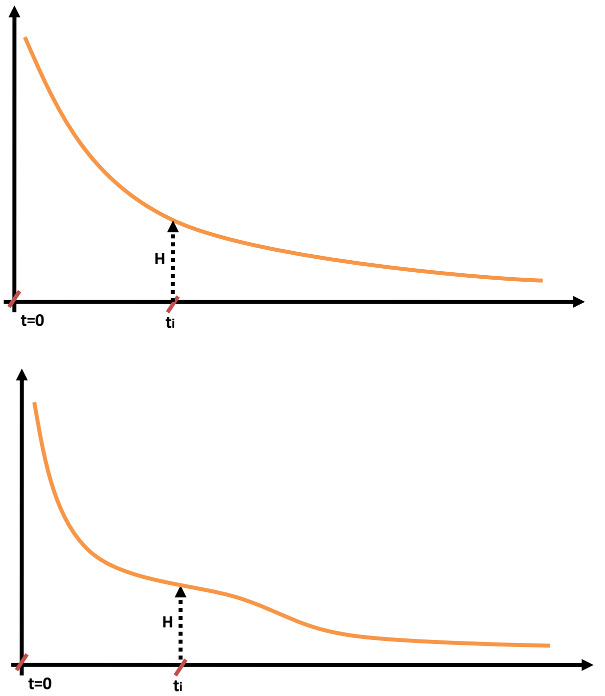

Figure 10. Heat retention at a sample points (a) Graph showing a typical point (b) Graph showing a point with resistance areas (typically top of a pocket)

Persistence Level

Persistence levels are measured by instances of time where heat at a certain point is still higher than a preset value μ. At the start heat is rapidly lost to a certain starting value λ. Following, heat persists through a certain time frame (shown in red onFigure 10). Persistence levels are computed using Equation 4.

$\mathrm{P} = \frac{t_i}{\tau}$; Where t_i is the time when heat drops below μ and is the RIMA computation step τ

Equation 4. Persistence Level

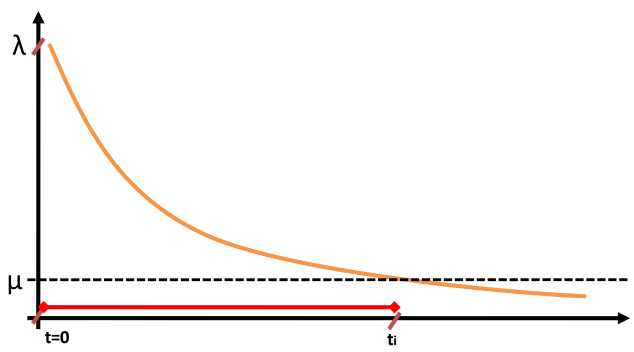

Figure 11. Persistence level shown in red

Persistence Value

Persistence values are measured by the incremental value of heat, until the time where heat drops lower than a preset value μ. It can be computed as the integral of the heat function or the area below the heat curve. Persistence value might sometimes better indicate persistence and refine the selection of tip points. Persistence values are computed using Equation 5.

$\mathrm{P} = \sum_{1}^{h_i<\mu} h_i$; Where h_i is the instantaneous value of heat.

Equation 5. Persistence Level

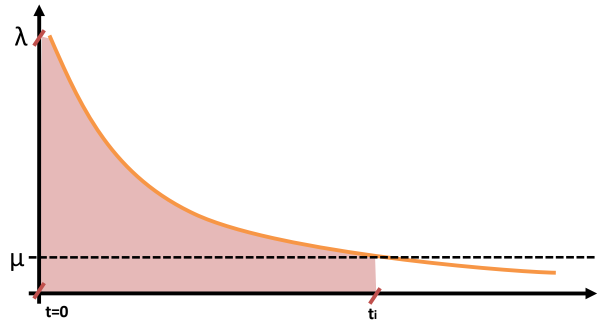

Figure 12. Persistence value (Area) shown in red

Stage 3: Persistence Clustering

The third stage will cluster points of similar persistence. The cloud of points is divided into subsets that group adjacent nodes having similar persistence values. Adjacency is determined from a connectivity matrix, which is a square matrix containing all nodes with a 1 when nodes are connected and 0 otherwise. Similarity in persistence applies when 2 nodes exhibit a heat value within a defined similarity percentage.

The clustering is to predict a mass behavior and to analyze the potential output. Typically elongated features will have 'rings'. The expected result would follow a typical heat analysis. To demonstrate, we illustrate the principle in Figure 13. The algorithm initiates clustering from the point persisting the most to dissipate heat. All points connected with persistence value higher than the matching limit, would be clustered together. When low similarity percentage is computed, features would be completely detected with surrounding elements and noise components. The result shown in step (a) would not be representative of any real feature. As the similarity percentage is increased, elongated rings (b) (c) and (d) becomes more distinctive. It is worthwhile to note that the tip of the feature might converge into one heated cluster or get further separated depending on the feature profile. This will be further detailed in stage 4.

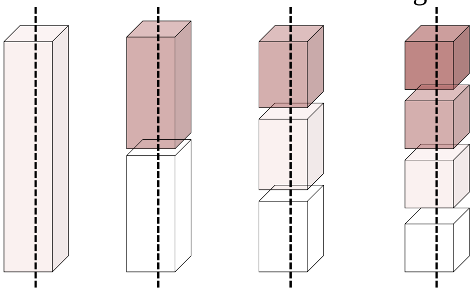

Figure 13. As persistence similarity increases, clustering is refined (a) low similarity (b) medium similarity (c) medium-high similarity (d) high similarity

Figure 14 shows an example of applying this persistence clustering stage. Section (a) represents the neutral cloud of point of our test part. Section (b) represents the clustering when a 80% similarity factor is applied. We can clearly note that the ‘tip’ of features is identified. The overall most resistant areas constitute the tips of the parts.

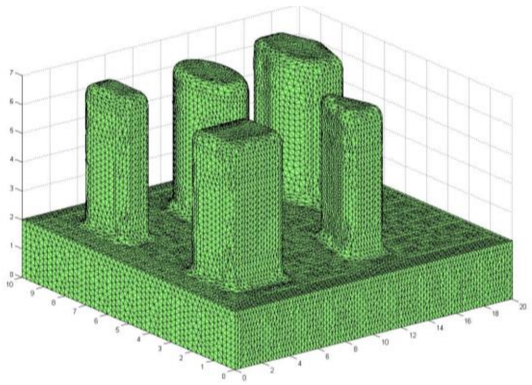

(a) Neutral

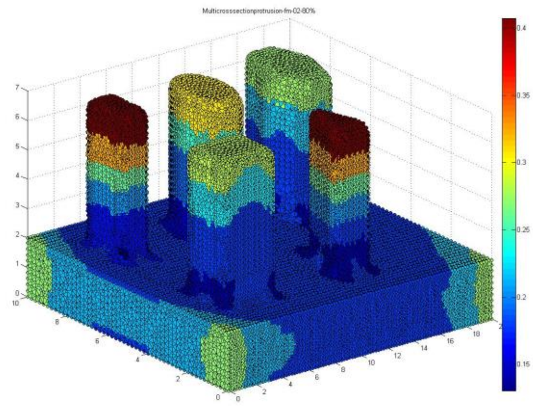

(b) 80% Similarity

Figure 14. Sample persistence clustering

Stage 4: Multiscale Filtering

This stage is the most important in the recognition step. We survey potential features through a multiscale filtering technique. The latter is used to separate clusters that form the features from other clusters. We use a methodology of separating cold bodies from warm bodies based on network graphs. The concept is to recognize and split feature islands. The latter is defined as the potential feature including the starting heated zone.

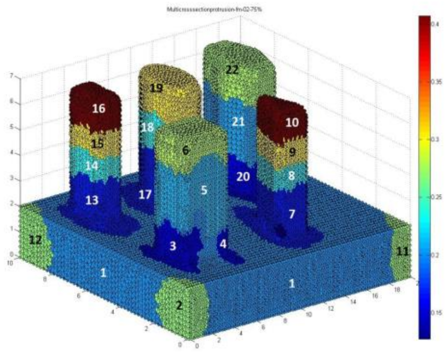

Figure 15. Identifying clusters and evaluating their average heat persistence

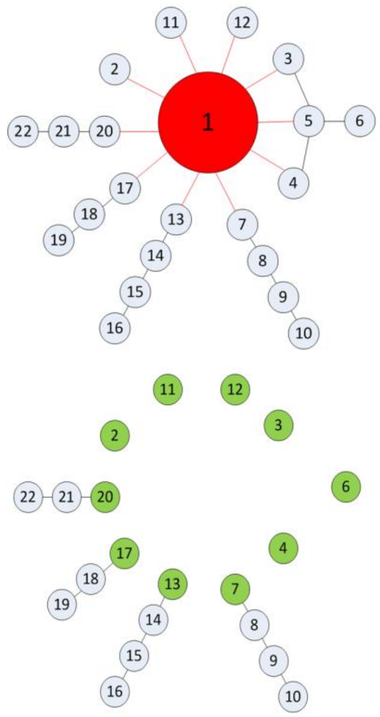

Figure 16. Splitting scheme for interconnected clusters

The multiscale filtering identifies at first the coldest weighted body. Figure 16 illustrates the concept. The concept is to find split islands by discarding interconnected subsets with more than 2 unidirectional flows. The scheme shows at first, that the coldest weighted body is identified, and following, it is discarded and all its connections are canceled. The new starting points are identified as the previous connections. Remaining new starting points are disabled (green) if they do not hold more than one directional flow. The algorithm continues until the last instance is validated. The output would also include meaningless clusters identified at a typically low similarity level (Figure 17).

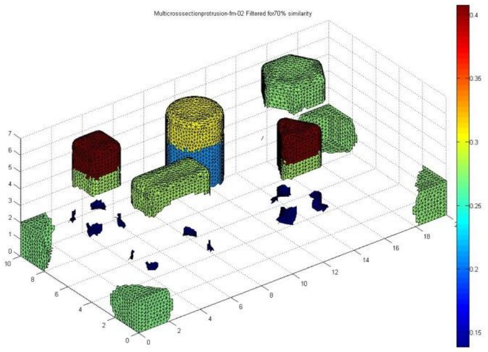

Figure 17. Sample result at 70% similarity

At this stage, the algorithm issues a merge request: It propagates the pre-identified tips and runs similarity and inclusivity tests for similar subsets at incremented persistence similarity subsets. The algorithm dynamically searches for the optimal clusters enclosing most pre identified sets.

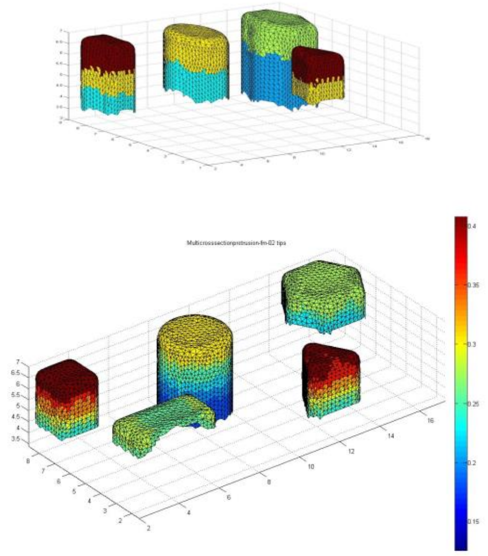

Figure 18. Final result of stage 4 following the application of the multiscale filtering.

Stage 5: Feature Recognition

The direction of a feature is determined by obtaining the line that best fits the points present in the cluster of clusters. The Singular Value Decomposition method was used to fit the points. The cross-section of a feature is determined by projecting the nodes of the cluster on a plane normal to the direction vector. After obtaining the clusters, the center of gravity of each cluster is computed. It was noticed that a similarity of 85% retains all necessary clusters after filtering. A lower percentage lead to missing clusters and a higher percentage lead to additional not needed clusters.

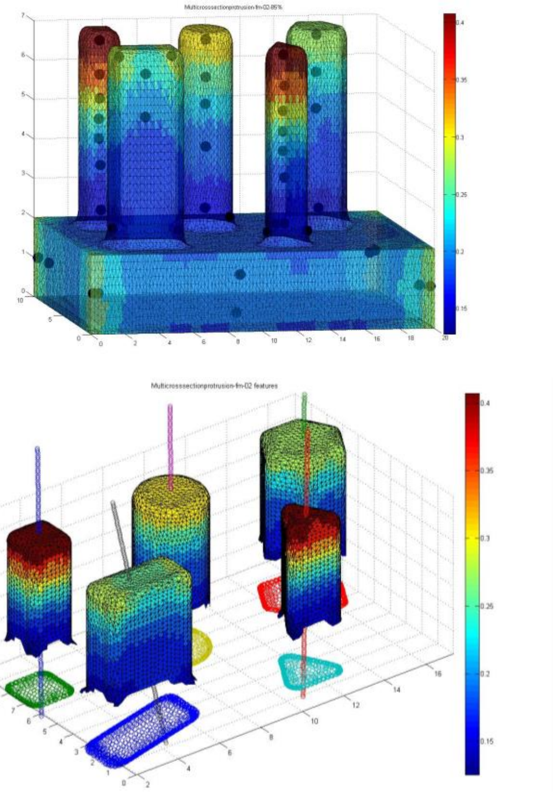

Figure 19. (a) cluster center of gravities (b) Recognized Features and attributes

4.2. Thinness probability

At this stage, we have the potential protrusion features already identified. Few stability errors of RIMA are still reported and are under investigation. This stage is an add-on that computes the thinness probability for identified features in a part, and classifies them.

The algorithm is composed of three stages: Point thinness, mean feature thinness, normalized thinness probability.

At the end of stage 1, we would have a group of identified features with the set of points belonging to them as well as the feature height. Following we would compute the point thinness defined by:

$$pt = Highest\left(\frac{Shortest\ connected\ distance}{Shortest\ distance}\right)$$

The shortest connected distance stands for the shortest path on the parts surface that connects two points. The shortest distance is the direct distance computation through the matter.

Once thinness is identified for every point, we compute the overall feature mean thinness which represents the average thinness value of the set of points defining the feature.

$$mt = average(pt)$$

Following, we calculate a normalisation value for every feature that is identified by:

$$n = \frac{Feature\ height}{shortest\ feature\ height}$$

The shortest feature height corresponds to the minimal value of feature height of the part.

Finally, the thinness value corresponds to:

$$thinness = n\,.\,mt$$

4.3. Current results

The following images present 4 case studies carefully selected to illustrate variable concepts such as different cross sections and different heights. The image shows as well the thinness values. The highest the value of thinness, the most likely a feature would be a thin feature.

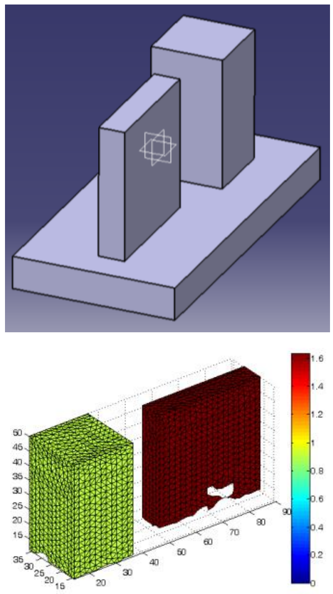

Figure 20. This part includes two protrusion features having different cross sections at the same height, the thinness probability clearly separated between them

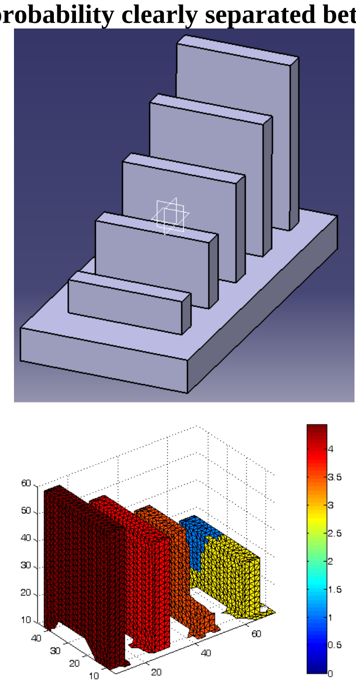

Figure 21. This part includes five protrusion features having similar cross sections at different height, the thinness probability clearly separated between them

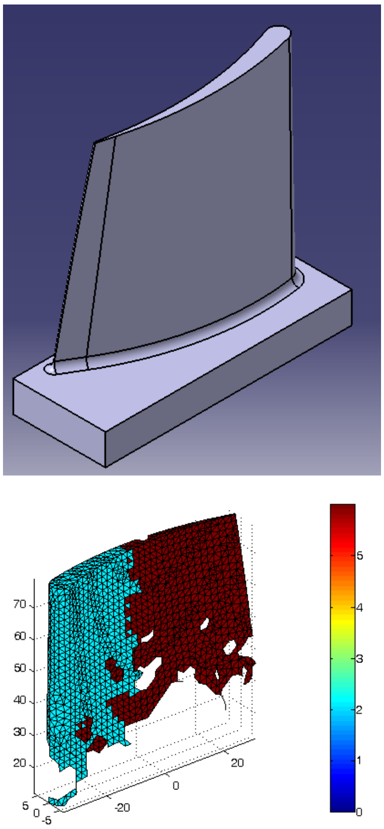

Figure 22. This airfoil was split into two thin zones, clearly showing the particular areas

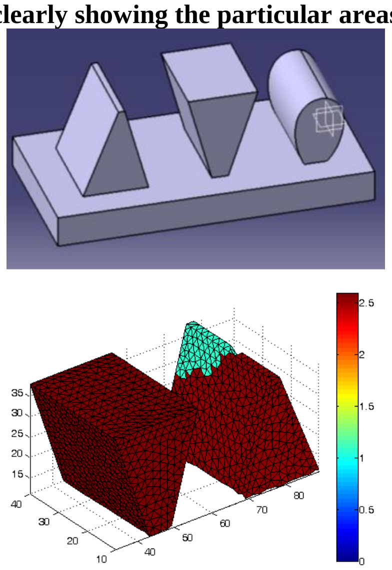

Figure 23. This part showed that the algorithm would generate the same thinness probability for reverse features. Note a minor feature recognition error at the tip of feature 2

5. CONCLUSION AND PERSPECTIVES

This paper presented a novel approach to detect thin features. The approach relies on combining persistence clustering and determining a thinness value. The current algorithm reorders all the identified features in a part from the most probable thin feature to the least probable. This would be presented to the process planner at the end of the design stage to confirm the selection and initiate particular manufacturing setup or to discard the selection.

The algorithm is still at its start, however it showed extreme stability when it comes to cross section variation as well as height variation. Following steps would include further refinement at the first step of feature recognition as well as treatment of parts with several complex features.

ACKNOWLEDGEMENT

The authors would like to acknowledge the contributions of Professor Karthik Ramani.

REFERENCES

[1] Harik, R., Durupt, A., Derigent W. and Ris, G., (2007), “Identification Des Entites Minces Pour La Fabrication"; Proceedings of the La Plagne AIP Primeca Conference

[2] Bravo, U., Alturazza, O., De Lacalle Lopez, L.N., Sanchez, J.A. and Campa, FJ., (2005), “Stability limits of milling considering the flexibility of the workpiece and the machine”, International Journal of machine Tool & Manufacture 45, 1669-1680

[3] Qiong, W., Yidu, Z. and Hongwei, Z., (2009) “Corner-milling of Thin Walled Cavities on Aeronautical Components”, Chineese Journal of Aeronautics 22, 677-684

[4] Rai, J. and Xirouchakis, P., (2008)“Finite element method based machining simulation environment for analyzing part errors induced during milling of thin-walled components”, International Journal of Machine Tools & Manufacture 48, 629-643

[5] HITHRU III, High-Throughput Production Processing Five-(5) Axis Titanium Components III, National Center for Manufacturing Sciences, Michigan, USA, August 2004

[6] Hirsh, J., Hajela, P., Spering, J.C., Coen, G.A. and Mytych, E., (2001) “Madesmart: An environment for Improved Development of Aircraft Components in Preliminary Design” Engineering with Computers 17, 162-185

[7] Harik, R., Derigent, W. and Ris, G., (2008) “Computer Aided Process Planning in Aircraft Manufacturing”, Computer-Aided Design and Applications 5, pp. 953

[8] Zhao, Z. and Shah, J.J., (2005) “Domain independent shell for DFM and its application to sheet metal

forming and injection molding", Computer Aided Design 37-9, pp 881-898

[9] Dissinger, T.E. and Magrab, E.B., (1996) "Geometric reasoning for manufacturability evaluation application to powder metallurgy", Computer-Aided Design 28-10, pp. 783-784

[10] A. Young, Eigenvalues and the Heat Kernel, 2003.

[11] M. Belkin, J. Sun, Y. Wang, Discrete Laplace Operator on Meshed Surfaces, Proceedings of the Annual Symposium on Computational Geometry, 2008, 278-287.

[12] T.K. Dey, K. Li, C. Luo, P. Ranjan, I. Safa, Y. Wang, Persistent Heat Signature for Pose-oblivious Matching of Incomplete Models, Eurographics Symposium on Geometry Processing, 29(5), 2010.

[13] Y. Fang, M. Sun, M. Kim, K. Ramani, Heat-Mapping: A Robust Approach Toward Perceptually Consistent Mesh Segmentation, Proceedings of the IEEE Computer Society Conference on Computer Vision and Pattern Recognition, 2011, 2145-2152.

[14] A. M. Bronstein, M. M. Bronstein, B. Busto, U. Castellani, M. Crisani, B. Falcidieno, L.J. Guibas, I. Kokkino, V. Murino, M. Ovsjanikov, G. Patané, I. Sipiran, M. Spagnuolo, J. Sun, SHREC 2010: Robust Feature Detection and Description Benchmark, Eurographics Workshop on 3D Object Retrieval, 2010.